

# End-to-End Learning-Based Ultrasound Reconstruction

Walter Simson<sup>\*1</sup>, Rüdiger Göbl<sup>\*1</sup>, Magdalini Paschali<sup>1</sup>, Markus Krönke<sup>2</sup>,  
Klemens Scheidhauer<sup>2</sup>, Wolfgang Weber<sup>2</sup>, and Nassir Navab<sup>1,3</sup>

<sup>1</sup> Technical University of Munich

<sup>2</sup> Nuclear Medicine, Klinikum rechts der Isar, Munich, Germany

<sup>3</sup> Johns Hopkins University, Baltimore, USA

**Abstract.** Ultrasound imaging is caught between the quest for the highest image quality, and the necessity for clinical usability. Our contribution is two-fold: First, we propose a novel fully convolutional neural network for ultrasound reconstruction. Second, a custom loss function tailored to the modality is employed for end-to-end training of the network. We demonstrate that training a network to map time-delayed raw data to a minimum variance ground truth offers performance increases in a clinical environment. In doing so, a path is explored towards improved clinically viable ultrasound reconstruction. The proposed method displays both promising image reconstruction quality and acquisition frequency when integrated for live ultrasound scanning. A clinical evaluation is conducted to verify the diagnostic usefulness of the proposed method in a clinical setting.

**Keywords:** Ultrasound Imaging · Clinical Evaluation · Reconstruction

## 1 Introduction

With the ubiquitization of deep learning (DL) methods in the medical community, statistical models learned by deep neural networks (DNNs) to improve medical imaging have received significant attention. Specifically in ultrasound (US) imaging, strides have been made in using DNNs to interpolate sub-sampled raw data in the case of MLT (a method used in cardiac US) [5], improve the filtering of received raw signals [1], and reconstruct US filtered images from sub-sampled raw data [3]. Lastly, [2] propose visualizing task-specific data from raw-signals in a binary contrast “alternative to beamforming” case. The implicit aim of all these approaches is to extract more information about the tissue being scanned from raw data than can currently be done from reconstructed ultrasound images. Though these approaches seem promising, to the best of our knowledge, until now there has been no DNN proposed to generate clinically viable full contrast ultrasound images—in terms of image quality and frame-rate—end-to-end from raw data by a DNN.

The reconstruction method most used in clinical US machines is delay and sum (DAS), due to its low computational complexity and data-independence.

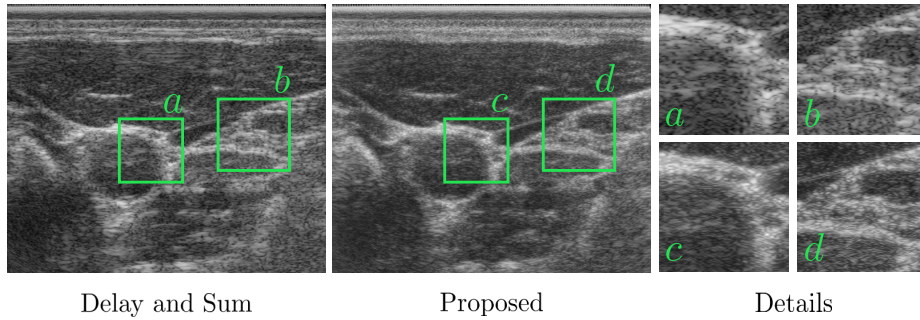


**Fig. 1.** Cross sectional scan of carotid artery. (left) DAS reconstruction (middle) the proposed reconstruction method. (right) Detail views.

On the other hand, data-dependent reconstruction algorithms such as minimum variance (MV) beamforming, can reconstruct ultrasound images of measurably higher quality, but are still too slow for routine clinical practice.

This dichotomy leads to the following problem: reconstruction algorithms with impressive quantitative results are prohibitively computationally intensive (i.e. low-frequency), whereas fast reconstruction algorithms are limited in image quality.

**Contribution:** We aim at bridging this gap; proposing a novel neural network based on a medical ultrasound specific loss function to reconstruct high quality and clinically relevant images. We propose an end-to-end learning-based data-dependent ultrasound reconstruction method for real-time applications.

For the general reader, the following sections briefly discuss the fundamentals of ultrasound imaging that motivate our method. Ultrasound experts can feel free to proceed to Section 2.1.

### 1.1 Ultrasound Raw Data

Scanline ultrasound imaging describes the process of transmitting and receiving focused ultrasonic beams from a number of ultrasound elements of a transducer. Its widespread use for anatomical imaging motivates learned receive beamforming for scanline imaging protocols. Raw data depicts the voltage measurements caused by the offsets of the piezo elements generated by the pressure wave-front in the tissue. After reception, the appropriate delays are applied to the individual channels to achieve dynamic receive focusing. These time-delayed raw data serve as the input for all of following reconstruction methods.

### 1.2 Delay and Sum

The most commonly used reconstruction method today is DAS. After dynamic receive focusing, the signals are multiplied with a constant weight vector (apodization), and summed together to get a local, depth-based signal intensity value.

The signal can be mathematically formulated as:

$$s_k(n) = \omega^T y_k(n) \quad (1)$$

where the signal of the  $k_{\text{th}}$  scanline  $s_k(n)$  is constructed by the multiplication of the apodization window vector  $\omega$  with the raw signal  $y_k$ [4].

### 1.3 Minimum Variance

Unlike DAS, MV beamforming is a data-dependent beamformer (also known as adaptive beamformer) that computes the apodization weights  $\omega$  based on statistics of the raw data in order to increase the signal-to-noise ratio (SNR) of the output image. This approach can be described as a maximization problem of signal-to-interference-plus-noise ratio (SINR) (c.f. Eq. 2), where  $R_k$  is the interference-plus-noise covariance matrix,  $\sigma_s^2$  is the signal power and  $a$  the steering vector [4].

$$\text{SINR} = \frac{\sigma_s^2 |\omega^T a|^2}{\omega^T R_k \omega}, \quad (2)$$

$$\underset{\omega}{\text{argmin}} \omega^T R_k \omega, \quad \text{where } \omega^T \mathbf{1} = 1 \quad (3)$$

Since in real-world situations the signal power  $\sigma_s^2$  is unknown, this problem is reformulated as a minimization problem of the denominator described in Eq. 3. Since this minimization problem must be solved for every reconstructed pixel, it has a high computational cost.

Our highly-parallelized MV beamformer achieves a reconstruction frequency of 0.14 Hz on an NVIDIA Titan V GPU. This low frame-rate motivates further reconstruction approaches, that are able to achieve real-time high-quality reconstructions. DNNs offer a potential solution to bridge this gap through a mapping from the space of raw ultrasound signals to the image space.

## 2 Method

We propose a new method of image reconstruction that allows near real-time reconstruction of ultrasound images while offering qualities of traditional state of the art methods.

### 2.1 Learning Beamforming

Training is performed with time-delayed raw data as a feature input and MV beamformed data as regression target. To address the challenging task of increasing the clinical efficacy of high-quality ultrasound reconstruction, a neural network is designed and trained to map raw data to image data.

**Training Data** As described in Sec. 1.1, time-delayed data is used as an input to the reconstruction. Time-delayed data ensures the spatial coherency of the 3-D raw input data, which is encoded to the channel dimension of the input.

The output target of the model is MV-beamformed data. Scan conversion is performed as a discrete subsequent step to ensure generalizability of the method. **Model Architecture** The proposed network is characterized by: (1) fully convolutional neural network (FCNN), (2) Encoder-decoder structure, (3) shallow depth, and (4) long- and short-term skip connections. The selection of a FCNN model allows for input size independence, which is required in ultrasound depending on the acquisition protocol and depth. Moreover, FCNNs offer accelerated computation due to the lack of their computationally intensive fully connected layers. Lastly, FCNNs map spatial relationships of the input data to output features, similarly to the process of MV-beamforming.

The encoder-decoder architecture ensures the highest informational density in the bottleneck layer. The network is kept shallow and only uses three convolutional blocks in the encoder and three in the decoder in order to optimize computation. Both the shallow network and batch normalization prevent overfitting. Lastly, the short-term skip connections within the dense convolutional blocks increase reconstruction accuracy and improve gradient flow. The long-term skip connection from the input to output passes on the fine-grained features from the raw data, such as speckle to the reconstructed image. In order to prevent data discontinuities on the edges of the data in the forward pass, an occurrence that is not found in ultrasound wave propagation, reflection padding is applied to the input raw data.

**Objective Function** The training loss functions combines the peak signal-to-noise-ratio (PSNR) loss, and the multi-scale structural similarity index (MS-SSIM) loss via a weighting factor  $\alpha$ . The PSNR loss  $\mathcal{L}_{\text{PSNR}}$  is based on the metric of the same name, which is widely used in the field of ultrasound and signal processing. It is accompanied by the MS-SSIM loss  $\mathcal{L}_{\text{MS-SSIM}}$  which serves as a measure for the perceived image reproduction[6]. The combined loss  $\mathcal{L}_{\text{US}}$  can then be formulated as:

$$\mathcal{L}_{\text{PSNR}} = 1 - \frac{10 \log_{10} \left( \frac{1}{\text{MSE}(x,y)} \right)}{\text{PSNR}_{\text{max}}} \quad (4) \quad \mathcal{L}_{\text{MS-SSIM}} = 1 - l_M \cdot \prod_{j=1}^M cs_j \quad (5)$$

$$\mathcal{L}_{\text{US}} = \alpha \mathcal{L}_{\text{MS-SSIM}} + (1 - \alpha) \mathcal{L}_{\text{PSNR}} \quad (6)$$

where  $\alpha$  is determined to be 0.75 through empirical experimentation.

## 2.2 Experimental setup

Reconstruction training is performed on an *in-vivo* data set acquired from five healthy volunteers, ages 23 - 59 (mean 32.4). In total, 3309 frames are used in the training and validation set with a four to one split between volunteers and five-fold cross-validation. A test set of two additional volunteers is used for final

**Table 1.** Reconstruction cross-validation comparison using different loss functions.

Loss Function	SSIM	PSNR
L1	$0.734 \pm 0.0105$	$24.3 \pm 0.610$
PSNR	$0.743 \pm 0.0128$	$24.2 \pm 0.790$
<b>PSNR-MSSSIM</b>	<b><math>0.749 \pm 0.009</math></b>	$24.2 \pm 0.487$

evaluation (1229 frames). The raw input data is cast from the discrete int16 values to float normalized between 0 and 1 to improve training dynamics. Training is performed on an NVIDIA Titan V GPU and all models are implemented in PyTorch. Training is performed with time-delayed raw data as a feature input and MV beamformed data as regression target, for 50 epochs with a learning rate of  $10^{-5}$ .

The inference run-time evaluation was performed on an NVIDIA Titan V GPU as well. The network is made compatible with libtorch for live inference. After training, the network weights and input data are cast to half-precision floats, along with the input data, to make use of the higher performance half-precision floating point units on NVIDIA GPUs. Inference is performed with the C++ interface of libtorch version 1.0.1.

### 3 Evaluation

Traditionally, ultrasound image quality is quantified by determining lateral and axial resolution, contrast-to-noise ratio (CNR), and the full width half maximum (FWHM). These measures are often used when evaluating new ultrasound reconstruction methods. Unfortunately, these metrics only take visualization of the reconstructed image into account, while disregarding the imaging frequency. Specifically, beamforming approaches such as MV are considered the gold standard in terms of image quality. However, they also suffer from impractical run-times preventing their use in clinical settings.

#### 3.1 Experimental Evaluation

We compare our method to the state of the art, w.r.t. the selected loss function, traditional image quality metrics, achieved frame-rate, and clinical acceptance.

A comparative evaluation of the proposed loss can be found in Table 1. The PSNR-MSSSIM loss performed best w.r.t. both mean and standard deviation of SSIM, exhibiting comparable PSNR. Consequently, we perform inference to generate evaluation images with the PSNR-MSSSIM loss. Figure 2 shows a qualitative comparison between reconstructions with DAS, MV, and our method. In the detail views, arrows point to regions where the reconstruction of fine anatomical structures is compared. The proposed reconstruction displays the least noise contamination around the indicated annular structure (right detail forearm). The same observation can also be made in the global view of the forearm scan.

**Table 2.** Classic ultrasound image quality measures determined using a CIRS 040GSE phantom. Our method was neither trained nor validated on phantom data.

	CNR [dB]	FHWm [mm]		Resolution [mm]	
		Axial	Lateral	Axial	Lateral
DAS	10.7	0.339	0.780	0.25	1.0
MV	9.30	0.326	0.301	0.25	1.0
Ours	8.68	0.332	0.425	0.44	1.0

In MV and our method, the border of the thyroid (lower detail images), as well as the vessel contained therein, are depicted more clearly.

For a direct quantitative comparison, we evaluate our method on wire and cyst phantoms (c.f. Table 2). Though all phantoms are unseen in both train and test sets, the proposed method performs comparably to MV. To investigate the imaging frequency of all considered algorithms, we perform live acquisitions and monitor the frame-rates. The resulting acquisition frequencies are 21 Hz, 0.14 Hz, and 17 Hz for DAS, MV and our reconstruction respectively.

### 3.2 Clinical Evaluation

Raw data acquisitions of the thyroid glands of volunteers are conducted by a trained nuclear medicine physician for clinical evaluation purposes. These include the gross anatomy and detailed views of thyroid nodules, both in transverse and axial views. Nodules are present in all three volunteers. Though our method is capable of real-time use, the DAS beamformer is used during all acquisitions in order to avoid bias.

Using DAS, selected frames with clinically relevant information are chosen offline by the acquisition physician. These frames are subsequently reconstructed with all considered methods and evaluated by four independent physicians; two male, two female, with 1, 3, 3, and 30+ years of clinical experience respectively.

Each physician is provided a series of 24 ultrasound image sets, similar to those in Fig. 2. Each set consists of three images in random order, all generated from the same raw channel data; one MV, one DAS and one image generated with our proposed method.

The physicians evaluate each of the images on seven qualitative metrics; contrast, image resolution, anatomy texture, overall image speckle, anatomy visibility (gross and fine), and the presence of artifacts in the image. All metrics are

**Table 3.** Results of clinical evaluation on a five-point scale

Metric	MV	DAS	Ours
Contrast	3.26	2.82	<b>3.35</b>
Texture	3.13	1.93	<b>3.14</b>
Speckle	<b>2.89</b>	1.78	<b>2.89</b>
Resolution	2.88	2.15	<b>2.95</b>
Gross anatomy	3.14	2.63	<b>3.18</b>
Fine anatomy	2.32	1.79	<b>2.47</b>
Artifact min.	<b>2.73</b>	2.26	2.67
Average	2.90	2.19	<b>2.95</b>

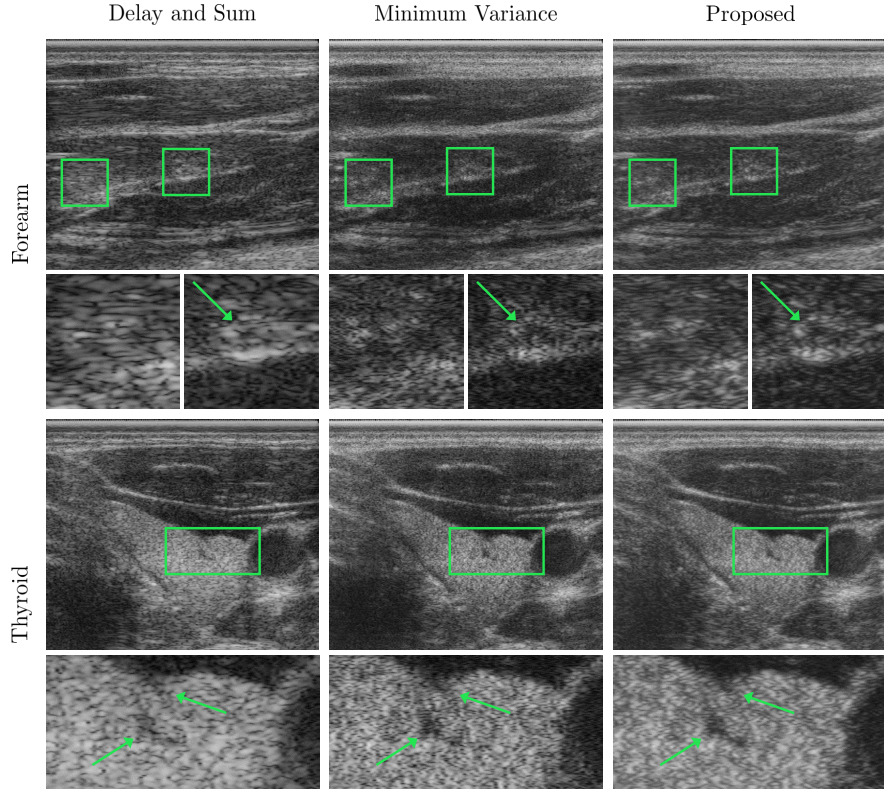


**Fig. 2.** Qualitative evaluation on two anatomies of unseen volunteers. (left) Delay and Sum, (center) Minimum variance, (right) our reconstruction. (top) supinated forearm, interior muscle (Brachioradialis), (bottom) thyroid cross-section.

rated on a five-point scale. Table 3 shows the average rating per metric and reconstruction method. The proposed method was rated highest in all categories, except artifact minimization, where it is only marginally outperformed by MV.

## 4 Discussion

Based on the evaluation of acquisition frequencies, we see that the proposed method with a frame-rate of 17 Hz offers a clinically viable reconstruction method. The qualitative results (c.f. Fig. 2) display a very promising visualization of fine anatomical structures in the reconstruction. This initial sign of promising *in-vivo* reconstruction quality is affirmed by the four physician evaluation.

Performance discrepancies on the phantom data (c.f. Table 2) can most likely be attributed to the fact that the network is only trained on *in-vivo* data. Augmenting the training set with non-organic data samples could prove to allow for more representative image quality metric evaluation. Similar to data-dependent

reconstructions, the perceptive field of the proposed method allows for “decisions” about local signal intensities to be derived from surrounding signal information. Thanks to the fully convolutional nature of the network, our method can be applied to images of arbitrary depths. Furthermore, properties of the images reconstructed by a DNN can be “steered” via the selection of an appropriate loss function and loss function regularizing term.

Lastly, the reported frame rate numbers show the immense potential for processing pipelines utilizing the advantages of neural networks to model complex behavior in competitive run-times. When the quality of MV and the proposed method are considered to be comparable, the proposed method offers a total speed-up of  $\frac{f_{\text{Ours}}}{f_{\text{MV}}} = \frac{17 \text{ Hz}}{0.14 \text{ Hz}} = 121$ .

## 5 Conclusion

Deep neural networks offer a promising alternative to high quality data-dependent beamforming methods. We have shown that gold standard approaches such as MV can be modeled by a DNN while offering substantial speed-up. Our clinical evaluation shows that physicians find the appearance of the proposed method visually pleasing and feel they can better extract clinically relevant information (c.f. Table 2). In this work, a new ultrasound reconstruction method is presented as an opportunity to bridge the gap between real-time beamformers and high-quality data-dependent beamformers. A suitable network architecture is defined and validated in both experimental and clinical contexts. By defining an ultrasound specific loss function to be used during training, images created with the proposed method can be steered towards relevant clinical objectives. We demonstrate the clinical feasibility of such an approach by integrating the trained network in an ultrasound device for real-time inference and *in-vivo* evaluation.

## References

1. Luchies, A., Byram, B.: Deep neural networks for ultrasound beamforming. *IEEE TMI* **37**(9), 2010–2021 (2018)
2. Nair, A., Tran, T., Reiter, A., Bell, M.L.: A deep learning based alternative to beamforming ultrasound images. pp. 3359–3363 (04 2018)
3. Simson, W., Paschali, M., Navab, N., Zahnd, G.: Deep learning beamforming for sub-sampled ultrasound data. In: 2018 IEEE International Ultrasonics Symposium (IUS). pp. 1–4 (Oct 2018). <https://doi.org/10.1109/ULTSYM.2018.8579818>
4. Szasz, T.: Advanced beamforming techniques in ultrasound imaging and the associated inverse problems. (Techniques avancées de formation de voies en imagerie ultrasonore et problèmes inverses associés). Ph.D. thesis, Paul Sabatier University, Toulouse, France (2016), <https://tel.archives-ouvertes.fr/tel-01506629>
5. Vedula, S., Senouf, O., Zurakhov, G., Bronstein, A.M., Zibulevsky, M., Michailovich, O.V., et. al.: High quality ultrasonic multi-line transmission through deep learning. In: MICCAI (2018)
6. Zhao, H., Gallo, O., Frosio, I., Kautz, J.: Loss functions for neural networks for image processing (2015), arXiv: 1511.08861